Journal of Bone Oncology 30 (2021) 100382

Contents lists available at ScienceDirect

Journal of Bone Oncology

journal homepage: www.elsevier.com/locate/jbo

Research Paper

Long-non-coding RNA RUSC1-AS1 accelerates osteosarcoma development by miR-101-3p-mediated Notch1 signalling pathway

Rui Jiang [a], Ziyan Zhang [b], Zhiwei Zhong [c], Chao Zhang [d,*]

[a] Department of Orthopedics, China-Japan Union Hospital of Jilin University, Changchun 130033, Jilin, China
[b] Department of Orthopedics, The Second Hospital of Jilin University, Changchun 130033, Jilin, China
[c] Department of Pain Medicine, China-Japan Union Hospital of Jilin University, Changchun 130033, Jilin, China
[d] Department of Ophthalmology, The Second Hospital of Jilin University, ChangchCun 130033, Jilin, China

ARTICLE INFO

Article history:
Received 30 December 2020
Revised 7 June 2021
Accepted 6 July 2021
Available online 16 July 2021

Keywords:
Osteosarcoma
RUSC1-AS1
miR-101-3p
Notch1
Progression

ABSTRACT

Background: Long non-coding RNA (lncRNA) RUSC1-AS1 has been found to modulate several cancers development. In this study, we explored the role of RUSC1-AS1 on osteosarcoma (OS) progression.
Methods: Quantitative Real-time PCR (qRT-PCR) was conducted to test the relative expression of RUSC1-AS1, Notch1 mRNA and miR-101-3p in OS tissues and adjacent normal tissues. Gain- or loss- of functional assays were carried out to determine the roles of RUSC1-AS1 and miR-101-3p in OS progression both *in vitro* and *in vivo*. The expression of E-cadherin, N-cadherin, Vimentin, Snail, Notch1, Ras and ERK was determined by Western blot. Furthermore, the relationships between RUSC1-AS1 and miR-101-3p, Notch1 and miR-101-3p were confirmed through RNA immunoprecipitation (RIP) and dual luciferase reporter gene assay.
Results: RUSC1-AS1 and Notch1 were up-regulated in OS cells and tissues. Down-regulating RUSC1-AS1 significantly attenuated the proliferative, epithelial-mesenchymal transition (EMT), growth, lung metastasis, migrative and invasive abilities of MG-63 and Saos-2 cells, and aggravated apoptosis, accompanied with down-regulated Notch1-Ras-ERK1/2 in those cells both *in vitro* and *in vivo*, while overexpression of RUSC1-AS1 exerted opposite effects. Overexpressing miR-101-3p in OS cells had similar effects as RUSC1-AS1 inhibition. In addition, RUSC1-AS1 functioned as a competing endogenous RNA (ceRNA) to competitively sponge miR-101-3p, thus upregulating Notch1 expression and mediating the malignant behaviors of OS cells.
Conclusion: RUSC1-AS1 is a novel oncogenic lncRNA in OS through the miR-101-3p-Notch1-Ras-ERK pathway, which might be a potential therapeutic target for OS.

1. Introduction

Osteosarcoma (OS), as one widespread bone malignancy [1], has high mortality among children and adolescents [2]. The high-dose chemotherapy was introduced about 35 years ago, while the OS survival rate has not improved since then [3]. Mounting researches have proved that long non-coding RNA (lncRNA) exerts a crucial effect in tumor occurrence and growth [4]. Therefore, the study of the molecular mechanism in OS is expected to provide a new therapeutic strategy.

Long non-coding RNAs (lncRNAs) have been proved to exert a prominent effect in a variety of biological processes such as proliferation, mobility, and apoptosis [5]. For example, lncRNA BE503655 was overexpressed in OS cell lines and its knockdown led to inhibitive ability of proliferation, invasion and migration [6]. LncRNA ZEB2-AS1 was upregulated in OS tissues and affects the proliferation, apoptosis, invasion, and metastasis of OS cells dependently through miR-107-SALL4 axis [7]. LncRNA RUSC1-AS1, a member of the lncRNA family, is located at 1q22 with a length of 3436 bp. Studies have shown that it is overexpressed in various cancers and is associated with worse prognosis. For instance, a high abundance of RUSC1-AS1 has been found in breast cancer (BCa) tissues. RUSC1-AS1 expression level was positively correlated with tumor size and clinical grades, and negatively correlated with BCa patients' overall survival. Silencing RUSC1-AS1 considerably inhibited the viability of MCF-7 and BT549 cells and

* Corresponding author at: Department of Ophthalmology, The Second Hospital of Jilin University, No.218 Ziqiang Street, Nanguan District, Changchun 130033, Jilin, China.
E-mail addresses: jr123@jlu.edu.cn (R. Jiang), zhangchao1984@jlu.edu.cn (C. Zhang).

https://doi.org/10.1016/j.jbo.2021.100382
2212-1374/

induced apoptosis [8]. However, the effect of RUSC1-AS1 in OS remains unknown.

MicroRNAs (miRNAs), as small non-coding RNAs, regulate gene expression at post-transcriptional level by suppressing mRNA translation or promoting mRNA degradation, and various physiological processes and pathologies are highly dependent on miRNAs [9,10]. miR-101-3p is a member of the miRNA family that regulates tumor growth and chemosensitivity in various cancers, including OS [11–13]. Interestingly, previous study revealed that miR-101-3p was negatively regulated by lncRNA DSCAM-AS1, which functioned as an oncogene in OS [14]. And lncRNA RUSC1-AS1 functions as a competing endogenous RNA of microRNA-744 and promotes tumorigenesis in cervical cancer [15]. However, little is understood about the RUSC1-AS1-miR-101-3p axis in OS.

As a classical signalling pathway, the Notch family that includes four Notch receptors (Notch 1, 2, 3, and 4) and five Notch ligands (Delta-like 1, 3, and 4 and Jagged1 and 2) has been identified to mediate multiple biological processes [16,17]. The Notch pathway becomes activated when Notch receptors and ligands interact [18]. In recent decades, more and more studies have stated that Notch1 upregulation implements in the carcinogenic initiation and development of various types of cancers. For example, downregulating Notch1 in aggressive prostate cancer cells decreases proliferation, invasion, tumorsphere formation and sensitizes prostate cancer cells to antiandrogen therapies [19]. While in T-cell acute lymphoblastic leukemia (T-ALL), miR-101 significantly repressed the proliferation and invasion, and induced potent apoptosis in Jurkat cells dependently through Notch1 pathway [20]. Interestingly, miR-139-5p functions as an anti-tumor gene in U2OS and MG63 cells by targeting the 3′UTR of Notch1 [21]. However, the mechanism of the RUSC1-AS1/miR-101-3p/Notch1 axis in OS remains elusive.

Here, we found the existence of a regulatory relationship between RUSC1-AS1 and miR-101-3p, miR-101-3p and Notch1 through bioinformatics. By detecting the expressions of RUSC1-AS1 and miR-101-3p, Notch1 in OS tissues and cells, we found that RUSC1-AS1, as a competitive endogenous RNA (ceRNA) of miR-101-3p, promotes the malignant behaviors of OS cells. In brief, this paper revealed a new molecular mechanism in OS growth and provided a new theoretical reference for its treatment.

2. Materials and methods

2.1. Collection and treatment of clinical specimens

The cancerous tissue and adjacent healthy tissues of 36 patients with primary OS who underwent OS resection in the Second Hospital of Jilin University from June 2015 to June 2016 were selected. The patients did not receive adjuvant therapy, such as chemotherapy and radiotherapy before the operation. The control group samples were from para cancer tissues of the same patient (at least 3 cm from the surgical margin). No cancer cells were found in the postoperative pathological examination. Later, all specimens were removed and immediately stored in liquid nitrogen at −196 °C until RNA was extracted. We followed all patients for 18 months to 30 months. Our experiments were approved by the Medical Ethics Committee of The Second Hospital of Jilin University with the informed consent of all participating patients.

2.2. Cell culture

Human osteoblasts hFOB1.19 and OS cell lines (MNNG/HOS, MG-63, S1353, U2OS, Saos-2, UMR-106) were purchased from ATCC (Rockville, USA). In RPMI-1640 complete medium containing 10% fetal bovine serum (FBS, Thermo Fisher Scientific, Shanghai, China) and 1% streptomycin (Thermo Fisher Scientific, Shanghai, China), these cells were cultured. Meanwhile, they were placed in an incubator at 37 °C with 5% CO_2 saturated humidity with the medium changed once every 2–3 days. When these cells approached fusion, they underwent 0.25% trypsinization (Thermo Fisher Scientific, Shanghai, China) and passage. It was found that RUSC1-AS1 expression was the lowest in the MG-63 cell line and the highest in the Saos-2 cell line. Therefore, MG-63 and Saos-2 became research objects in subsequent studies.

2.3. Cell transfection

Saos-2 cells and MG-63 cells were seeded in 24-well plates. SiRNA (si-RUSC1-AS1) or of RUSC1-AS1 overexpression plasmids, Notch1 overexpression plasmids, or their negative controls (100 nM, GenePharma, China) were respectively transfected into Saos-2 cells and MG-63 cells to establish the RUSC1-AS1 knockdown or overexpression model. miR-101-3p mimics and the corresponding negative control (NC) (Guangzhou Ribobio) were used to induce miR-101-3p overexpression model. Lipofectamine 2000 reagent (Sangon Biotech) was applied for transfection. 24-hour after transfection, the culture was exchanged with new fresh medium and the cells were continuously incubated for 24 h. Then qRT-PCR was performed to detect RUSC1-AS1, Notch1 and miR-101-3p to ensure the transfection efficiency.

2.4. qRT-PCR

The expressions of RUSC1-AS1, miR-101-3p, and Notch1 in MNNG/HOS, MG-63, S1353, U2OS, Saos-2, and UMR-106 cells were evaluated by real-time quantitative polymerase chain reaction (qRT-PCR). Following the manufacturer's guidelines, the total RNA was extracted from the cultured cells with TRIzol reagent (Invitrogen, Carlsbad, CA). Then, lncRNA and mRNA were reverse-transcribed into the first strand of complementary DNA (cDNA) by using the reverse transcription kit Thermo (purchased from Thermo Fisher Scientific). Further, the microRNA first-strand cDNA synthesis package (Sangon Biotech, Shanghai, China) was employed to the reverse transcription process for miRNA analysis. We used the SYBR-green PCR Master Mix Kit (Applied Biossystems, Foster City, CA) and the TaqMan miRNA analysis Kit (Applied Biossystems) to respectively amplify RUSC1-AS1, Notch1, and miR-101-3p. All amplifications were performed on the 7900HT rapid real-time system (Applied Biosystems). We took GAPDH as endogenous control and used $2^{-\Delta\Delta Ct}$ method to analyze the relative expressions of RUSC1-AS1 and Notch1, while U6 was for miR-101-3p. The primer sequences are: RUSC1-AS1, forward, 5′-CAGGGTCCCACTATGTTGCT-3′ reverse, 5′- CCATTTTATAGGCGGGGAGT-3′; miR-101-3p, forward, 5′- GCCGCCACCATGGTGAGCAAGG-3′ reverse, 5′- AATTGAAAAAAGTGATTTAATTT-3′; U6, forward, 5′- CTCGCTTCGGCAGCACATA-3′ reverse, 5′- CTCGCTTCGGCAGCACATA-3′; Notch1, forward, 5′- CAACATCCAGGACAACATGG-3′ reverse, 5′- GGACTTGCCCAGGTCATCTA-3′; GAPDH, forward, 5′-CGCTGAGTACGTCGTGGAGTC-3′, reverse, 5′-GCTGATGATCTTGAGGCTGTTGTC-3′.

2.5. CCK8 method

MG-63 and Saos-2 cells in the logarithmic growth phase went through 0.25% trypsinization and were made into a single-cell suspension. After calculation, the cells were vaccinated in 96-well plates (about 2000 cells per hole) and incubated for 24 h, 48 h, 72 h (37 °C, 5% CO_2). Then, the incubation was continued for 2 h with the addition of 10 μl CCK8 reagent (Beyotime, Shanghai, China) in each well. Finally, the absorbance value of each hole

was detected with the enzyme standard device under 450 nm wavelength.

2.6. BrdU method

MG-63 and Saos-2 cells were seeded in 24-well plates. After 24 h, they were added with 10 μmol/L BrdU (Beyotime, Shanghai, China) during the logarithmic proliferation phase for 2 h. After denaturing the cells, BrdU primary antibody (ab8152, 1: 100, Abcam, Shanghai, China) was added and incubated for 2 h at room temperature. Next, with the addition of fluorescent secondary antibody, the cells underwent another 2-hour incubation at room temperature. Finally, we labeled the nucleus with 10 μmol/L Hoechst33342 (Beyotime, Shanghai, China) and took photographs using a fluorescent inverted microscope and performed statistical analysis.

2.7. Wounding healing assay

The MG-63 and Saos-2 cells in the logarithmic growth phase were spread in a 6-well culture plate at 1×10^6/ml. When the cells reached 80% to 90% confluence, a scratch was drawn with a sterile tip perpendicular to the cells as much as possible. Then, the cells went through three times PBS wash to remove floating cells, added with DMEM medium containing 2.5% fetal bovine serum, placed 24-hour in an incubator (37 °C, 5% CO_2), secured with 4% paraformaldehyde and measured the scratch width under a microscope after 24-hour incubation. The scratch width represented its migration ability.

2.8. Transwell assay

After 24-hour transfection, the cells underwent trypsinization passage, collected, resuspended in serum-free RPMI1460 complete medium with a cell density of 1×10^5/ml. Then, we inoculated them in Transwell upper chamber (8 μm pore size membrane) with 500 μl RPMI-1460 complete medium containing 10% PBS in the lower chamber and cultured them for 6 h. We used a cotton swab to wipe off the unmigrated cells on the membrane and secured the cells migrated and adhered to the lower chamber with 4% paraformaldehyde for crystal violet staining. At high magnification, 5 representative microscopic fields on the membrane were randomly selected to count the number of membrane-penetrating cells, and the mean values of 3 replicates were taken to represent tumor cell invasive ability.

2.9. Western blot

After cell treatment, we discarded the culture medium, added protein lysate (Roche) and isolated total protein. Then, 50 μg total protein was added to 12% polyacrylamide gel for 2-hour electrophoresis at 100 V. Later, they were transferred electrically to polyvinylidene fluoride (PVDF) membranes. Afterwards, the membranes were sealed with 5% defatted milk powder (1 h, at room temperature), washed with TBST (3 times, 10 min each) and incubated with primary antibodies including anti-Notch1 (Abcam, ab52627, diluted concentration 1:1000, MA, USA), anti-E-cadherin (Abcam, ab40772, diluted concentration 1:1000, MA, USA), anti-Vimentin (Abcam, ab8978, diluted concentration 1:1000, MA,USA), anti-N-cadherin (Abcam, ab76011, concentration 1:1000, MA, USA), anti-Snail (Abcam, ab180714, concentration 1:1000, MA, USA), Ras (Abcam, ab52939, concentration 1:1000, MA, USA), anti-ERK1/2 (Abcam, ab184699, concentration 1:1000, MA, USA), anti-ERK1 (phospho T202) + ERK2 (phospho T185) (Abcam, ab201015, concentration 1:1000, MA, USA) overnight at 4 °C. Afterwards, the membranes were rinsed with TBST and incubate with horseradish peroxidase (HRP) labeled anti-rabbit secondary antibody (Abcam, ab150117, dilution of 1:2000, MA, USA) (1 h, room temperature). Next, we rinsed the membranes three times with TBST for 10 min each time. Eventually, western blot special reagent (Invitrogen) was used for color imaging and Image J was employed to analyze the gray value of each protein.

2.10. Dual luciferase reporter gene assay

All luciferase reporter vectors (RUSC1-AS1-WT, RUSC1-AS1-MUT, Notch1-WT, Notch1-MUT) were constructed by Promega (Madison, WI, USA). RUSC1-AS1-WT and Notch1-WT contained the binding sites with miR-101-3p, while RUSC1-AS1-MUT and Notch1-MUT was mutant for the binding sites with miR-101-3p. MG-63 cells (4.5×10^4) were inoculated in a 48-well plate and cultured till 70% confluent. Then, the vectors including RUSC1-AS1-WT, RUSC1-AS1-MUT, Notch1-WT and Notch1-MUT were co-transfected with miR-101-3p mimics or negative control with lipofectamine 2000 into MG-63 cells. After 48 h transfection, the luciferase activity was evaluated following to the manufacturer's guidelines. We made all experiments in triplicate and repeated them three times.

2.11. RIP assay

MG-63 and Saos-2 cells were transfected with miR-101-3p mimics and miR-NC, respectively. RIP analysis was performed on these transfected cells by using the Magna RIPTM RNA binding protein immunoprecipitation kit (Millipore, Bedford, MA, USA) 48 h after transfection. Afterwards, the cells went through incubation with anti-Ago2 antibody (Millipore) or negative control IgG (Millipore), and the relative enrichment of RUSC1-AS1 and Notch1 was examined via qRT-PCR.

2.12. Tumor formation in nude mice

We took OS cells MG-63 and Saos-2 in logarithmic growth phase and adjusted cell concentration to 2×10^6 ml-1. The nude mouse was injected with 0.1 ml cell suspension (containing 2×10^6 cells) into the subcutaneous axilla of the left forelimb and observed for tumor growth (n = 4 in each group). The tumor volume was measured at 7 d, 14 d, 21 d, 28 d, 35 d and 42 d after subcutaneous injection, respectively. The nude mice were sacrificed after 42 days. For evaluating the metastasis of OS cells, OS cells MG-63 and Saos-2 transfected with RUSC1-AS1 overexpression plasmids or Si-RUSC1-AS1 or their negative controls were injected into the tail vein of nude mice. 6 weeks later, the lung of each nude mice was isolated and subjected to histopathological examination for evaluating the number of pulmonary metastases. The tumor tissues in each group were completely stripped and the tumor weight was accurately measured. All nude mice were sacrificed before they got euthanasia via intraperitoneal injection with pentobarbital sodium (150 mg/kg). We examined the ascites presence and the lungs carefully and observed the tumor lung metastases status.

2.13. Immunohistochemical (IHC) staining

The expression of Notch1 and Vimentin in the tumor issues was detected by Immunohistochemical (IHC) staining. Briefly, the tissues of the xenograft tumors in each experimental group were collected and fixed by in 4% paraformaldehyde for 2 days, embedded in paraffin. After antigen retrieval was performed, and 1% bovine serum albumin (BSA) was used to block with the sections for 20 min, then incubated with primary rabbit anti-Notch1 polyclonal antibody (Abcam, ab52627, 1:200, MA, USA) or anti-Vimentin

(Abcam, ab8978, diluted concentration 1:200, MA,USA) at 4 °C overnight. Next, the sections were incubated with HSP-labeled Goat Anti-Rabbit IgG H&L (ab205718, Abcam, 1:500, MA, USA) at room temperature for 30 min. Later, the slides were counterstained with hematoxylin. The images were taken with the Nikon digital camera system in combination with Olympus microscopy.

2.14. Flow cytometry

The OS cells MG-63 and Saos-2 were collected using 0.25% trypsin (1 ×). Then they were rinsed with ice-cold phosphate-buffered saline (PBS) for three times. The Annexin V-Fluorescein Isothiocyanate (FITC) Apoptosis Detection Kit (Biolegend, San Diego, CA, USA) was utilized to test the apoptotic rate of the cells. Briefly, 100 μl of binding buffer was used to resuspend the cells, and 5 μl of Annexin V-FITC and 5 μl of the propidium iodide solution were then added into the cell suspension. After a 20-min incubation at 37 °C in darkness, the proportion (%) of apoptotic cells was assessed on a flow cytometer (FACScan™; BD Biosciences, Franklin Lakes, NJ, USA).

2.15. Statistical analysis

SPSS17.0 statistical software (SPSS Inc., Chicago, IL, USA) and the mean ± standard deviation (x ± s) was taken for data analysis. Correlation test was analyzed by Pearson linear regression analysis. One-way analysis of variance was carried out for the multi-group comparison, and an independent-sample *t*-test was taken for comparison between the two groups. P < 0.05 was considered as statistically meaningful.

3. Results

3.1. RUSC1-AS1 and Notch1 levels were increased in OS tissues and cells

We conducted qRT-PCR to verify RUSC1-AS1 and Notch1 levels in OS tissues. The results illustrated that RUSC1-AS1 and Notch1 expressions in OS tissues were remarkably up-regulated compared with the adjacent normal tissues (P < 0.05, Fig. 1 A, B). The clinical correlation analysis manifested that the higher level of RUSC1-AS1 was related with higher Enneking stages, larger tumor size and positive distant metastasis of OS patients (P < 0.05, Table 1). Additionally, western blot results also confirmed that Notch1 was upregulated in OS tissues compared with adjacent normal tissues (P < 0.05, Fig. 1C). Pearson analysis showed that RUSC1-AS1 and Notch1 were positively correlated in OS tissues (P < 0.05, Fig. 1D). Besides, we also examined RUSC1-AS1 and Notch1 expressions in different OS cell lines via qRT-PCR or western blot. The results demonstrated that both of RUSC1-AS1 and Notch1 mRNA and protein expressions were enhanced in OS cell lines (MNNG/HOS, MG-63, S1353, U2OS, Saos-2, UMR-106) compared with human osteoblasts hFOB1.19 (P < 0.05, Fig. 1E–G). Therefore, these results only indicated both RUCS1-AS1 and Notch1 are upregulated in OS and may have a role in osteosarcomagenesis.

Table 1
The relationship between RUSC1-AS1 expression level and clinical characteristics in OS (OS) patients.

Characteristics	Patients	Expression of lncRNA RUSC1-AS1		P-value
		Low RUSC1-AS1 level	High RUSC1-AS1 level	
Total	36	18	18	
Age(years)				0.735
＜18	21	11	10	
≥18	15	7	8	
Gender				0.171
Male	22	13	9	
Female	14	5	9	
Pathological				0.126
G1	4	3	1	
G2	14	9	5	
G3-G4	18	6	12	
Enneking stage				0.044*
Ⅰ-ⅡA	16	11	5	
ⅡB- Ⅲ	20	7	13	
Tumor size				0.015*
＜8cm	23	15	8	
≥8cm	13	3	10	
Distant metastasis				0.035*
Yes	7	2	5	
No	29	16	13	

Note: * represents p < 0.05.

3.2. RUSC1-AS1 promoted the malignant behaviors of OS cells

For the analysis of RUSC1-AS1 effect on OS cell line (MG-63 and Saos-2) proliferation, migration, and invasion, over-expressed and

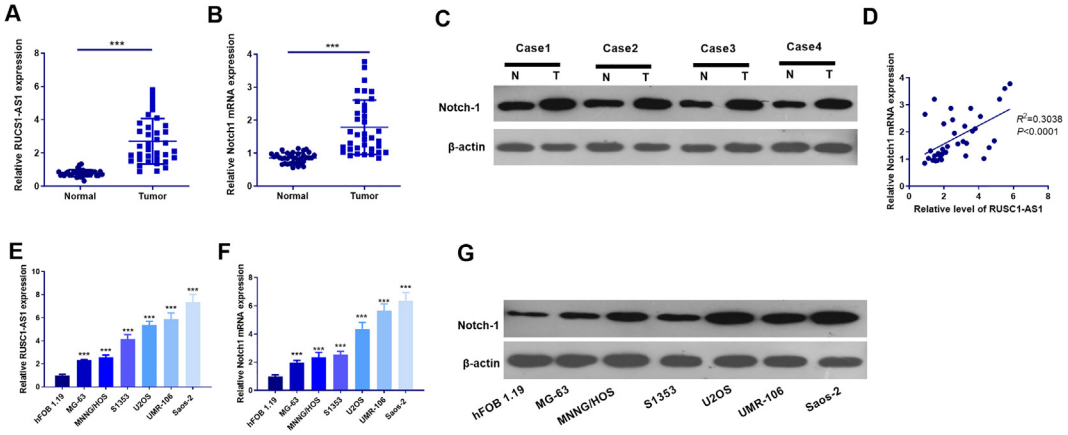

Fig. 1. RUSC1-AS1 and Notch1 were up-regulated in OS tissues and cells. A and B: qRT-PCR was taken to evaluate RUSC1-AS1 and Notch1 expressions in OS tissue and adjacent tissues, respectively. *** P < 0.001 (vs. Normal group). C. Western blot was used to detect Notch1 expression in four pairs of OS tissues (T) and the adjacent normal tissues (N). D: Pearson analysis illustrated the relationship between RUSC1-AS1 and Notch1 in OS. R^2 = 0.304, P < 0.0001. E and F: RUSC1-AS1 and Notch1 expressions in normal osteoblasts and OS cell lines were examined via qRT-PCR, respectively. ** P < 0.01, *** P < 0.001 (vs.hFOB 1.19 group). G. Western blot was used to detect Notch1 expression in normal osteoblasts and OS cell lines.

downregulated RUSC1-AS1 cell models were established in MG-63 and Saos-2 cell lines (Fig. 2A). Next, we evaluated the malignant behaviors of OS cells. BrdU assay and CCK8 assay illustrated that, OS cell proliferation was enhanced with RUSC1-AS1 overexpression but repressed when RUSC1-AS1 was knocked down ($P < 0.05$ vs. Vector group or Si-NC group, Fig. 2B–D). The apoptosis rate of the OS cells was examined by flow cytometry, which showed that RUSC1-AS1 upregulation attenuated cell apoptosis, while RUSC1-AS1 knock-out promoted cell apoptosis ($P < 0.05$ vs. Vector group or Si-NC group, Fig. 2E). Further, wounding healing assay and Transwell assay were performed to test cell migration and invasion, respectively. It as found that compared with the Vector group or Si-NC group, the increased RUSC1-AS1 markedly enhanced the OS cell migration and invasion, while RUSC1-AS1 knockdown considerably decreased OS cell migration and invasion ability. ($P < 0.05$, Fig. 2F and G). EMT-related proteins were measured via western blot. The results indicated that after RUSC1-AS1 upregulation, the level of epithelial marker E-cadherin was decreased and the level of interstitial markers N-cadherin, Vimentin and Snail were increased. After RUSC1-AS1 was downregulated, the epithelial marker E-cadherin was enhanced and the level of interstitial markers N-cadherin, Vimentin and Snail

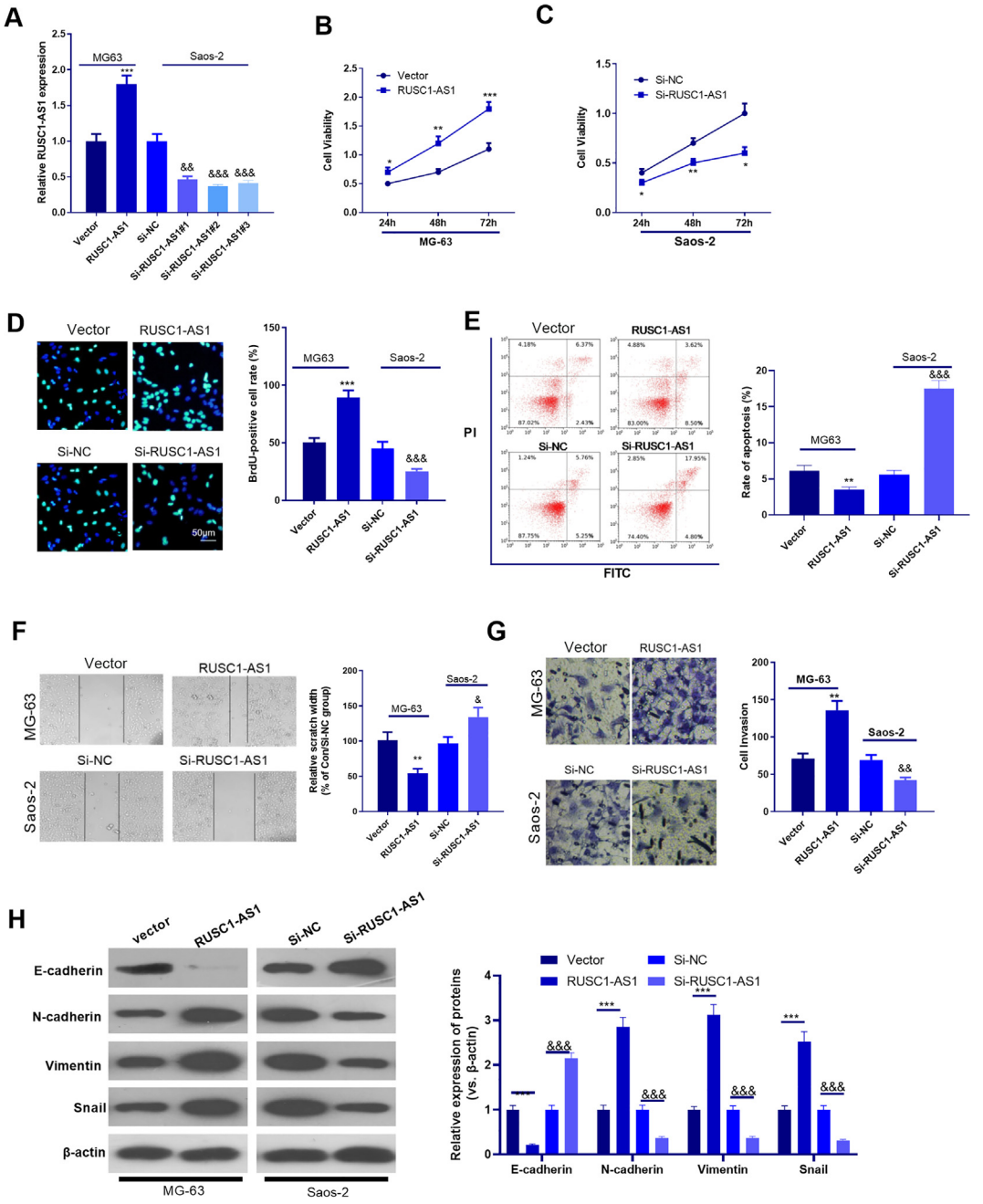

Fig. 2. RUSC1-AS1 promoted OS cell proliferation, migration and invasion and inhibited apoptosis. A: Establishment of RUSC1-AS1 overexpression and knockdown models in OS cell line MG-63 and Saos-2, respectively. RUSC1-AS1 overexpression plasmids were transfected into MG-63 cells, and Si-RUSC1-AS1 was transfected into Saos-2 cells. qRT-PCR was performed to detect RUSC1-AS1. B-D: CCK8 assay (B, C) and BrdU assay (D) were performed to detect cell proliferation. E. The apoptosis rate of the cells was examined by flow cytometry. F and G. Wounding healing test (E) and Transwell assay (F) for migration and invasion determination. H: The EMT markers including E-cadherin, N-cadherin, Snail and Vimentin were examined via Western blot. * $P < 0.03$, ** $P < 0.01$, *** $P < 0.001$ (vs. Con group). & $P < 0.05$, && $P < 0.01$, &&& $P < 0.001$ (vs. Si-NC group). N = 3.

were restrained (Fig. 2H). These statistics suggested that RUSC1-AS1 promotes the malignant phenotypes of OS cells and exerts a carcinogenic effect.

3.3. RUSC1-AS1 accelerated OS cells growth and EMT in vivo

For identifying the role of RUSC1-AS1 in OC cell growth, we performed xenografted tumor model in nude mice using MG-63 with RUSC1-AS1 overexpression and Saos-2 with RUSC1-AS1 knockdown. The volume of tumor nodes was calculated. At the 6th week after tumor cell transplantation, the mice were sacrificed and the formed tumor were isolated. We found that compared with the Vector group, forced RUSC1-AS1 upregulation enhanced tumor volume and size. However, the downregulation of RUSC1-AS1 significantly reduced tumor volume and size ($p < 0.01$, compared with Si-NC group, Fig. 3A–D). We also measured tumor weight and found that RUSC1-AS1 overexpression enhanced tumor weight. On the contrary, Si-RUSC1-AS1 in Saos-2 cells attenuated the tumor weight of nodes (Fig. 3E). Western blot was then used to detect the EMT markers in the formed tumor nodes. As shown in Fig. 3E, MG-63 cells with amplified RUSC1-AS1 had lower level of E-cadherin, but higher levels of N-cadherin, Vimentin and Snail. However, downregulation of RUSC1-AS1 increased E-cadherin and decreased N-cadherin, Vimentin and Snail expression (Fig. 3F). The result of ICH also confirmed that RUSC1-AS1 upregulation promoted Vimentin expression in the tumor tissues, and RUSC1-AS1 knockdown repressed Vimentin expression ($p < 0.01$ vs. Vector or Si-NC group, Fig. 3G–H). Additionally, we performed lung metastasis experiment in the nude mice. Our data suggested that overexpression of RUSC1-AS1 in MG-63 cells enhanced the pulmonary metastases and RUSC1-AS1 knockdown had the opposite effects ($p < 0.05$ compared with Vector or Si-NC group, Fig. 3I). These results further demonstrated that RUSC1-AS1 promotes OS cell proliferation, EMT and pulmonary metastases *in vivo*.

3.4. RUSC1-AS1 promoted Notch1 expression and activated Ras-ERK pathway

For exploring the downstream mechanism of RUSC1-AS1, qRT-PCR and WB was performed to determine Notch1 and Ras-ERK levels. As the data showed, RUSC1-AS1 overexpression promoted Notch1 mRNA level in MG-63 cells. However, the knockdown of

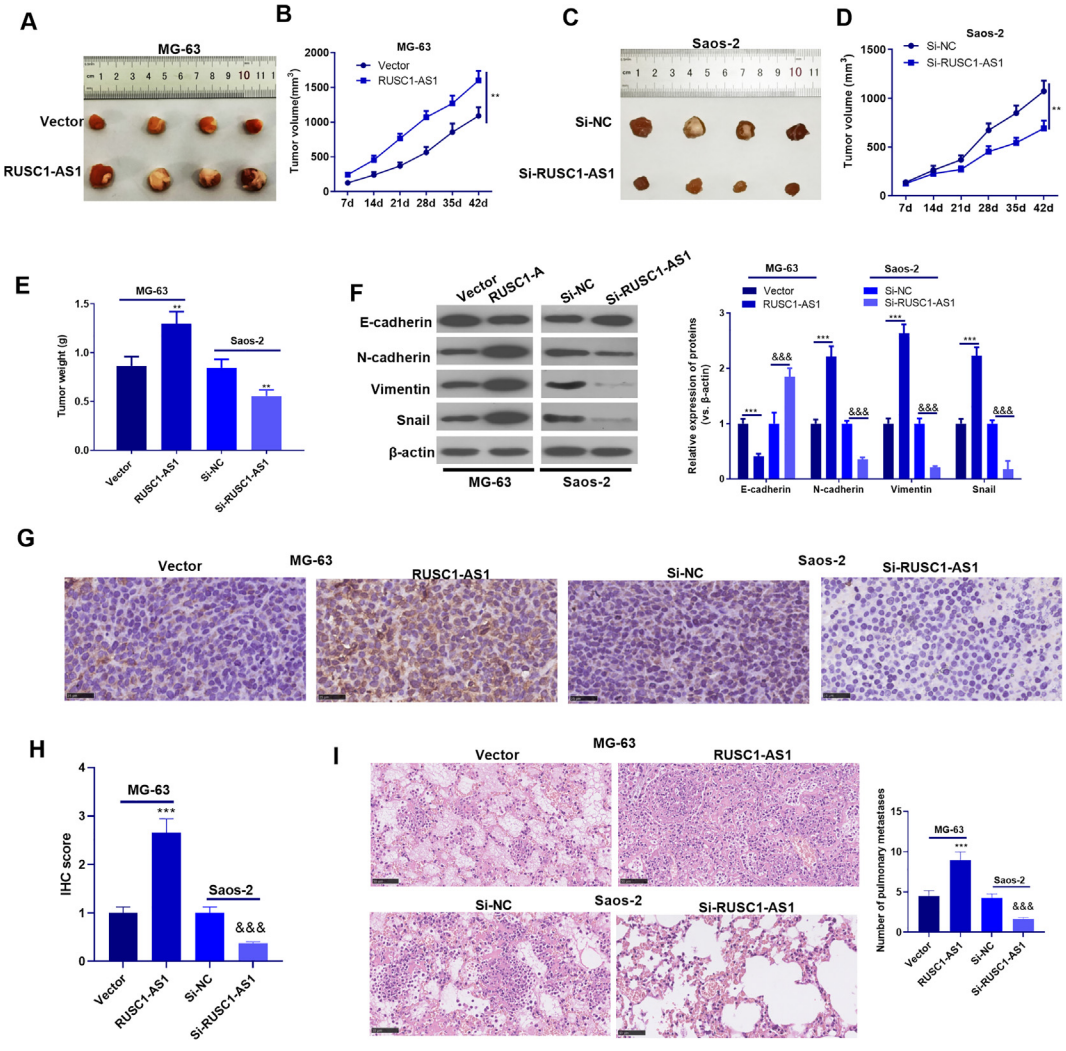

Fig. 3. RUSC1-AS1 promoted tumor cell growth *in vivo*. MG-63 cells transfected RUSC1-AS1 overexpressing plasmids and Saos-2 cells transfected with Si-RUSC1-AS1 were subjected to xenograft experiments. A and C: Tumor images in the fifth week. B and D: Tumor volume during five weeks of incubation was calculated. E:Tumor weight during five weeks of incubation. ** $P < 0.01$ (vs. Vector group or Si-NC group). F: The EMT markers including E-cadherin, N-cadherin, Snail and Vimentin in the tumor tissues were examined via Western blot. G-H:IHC was used for detecting Vimentin in the formed tumor tissues. I. RUSC1-AS1 overexpression plasmids or Si-RUSC1-AS1 or their negative controls were injected into the tail vein of nude mice. 6 weeks later, the lung of each nude mice was isolated and subjected to HE-staining examination for evaluating the number of pulmonary metastases. ** $P < 0.01$, *** $P < 0.001$ (vs. Vector group), && $P < 0.01$, &&& $P < 0.001$ (vs. Si-NC group). N = 4.

RUSC1-AS1 attenuated Notch1 mRNA level in Saos-2 cells (Fig. 4A). In addition, the western blot results suggested that overexpressing RUSC1-AS1 enhanced the Notch1, Ras and phosphorylated ERK1/2 in MG-63 cells. However, suppressing RUSC1-AS1 mitigated Notch1, Ras and phosphorylated ERK1/2 levels in Saos-2 cells (Fig. 4B). What's more, qRT-PCR, IHC and Western Blot were conducted to evaluate Notch1, Ras or ERK1/2 in the tumor tissues. It was found that the RUSC1-AS1 group had higher expression of Notch1, Ras and phosphorylated ERK1/2(compared with Vector group), and Si-RUSC1-AS1 had lower level of Notch1, Ras and phosphorylated ERK1/2 (compared with Si-NC group, Fig. 4C, D). Hence, RUSC1-AS1 might promote the malignant behaviors of OS cells via increasing the expression of Notch1 and activating Ras-ERK pathway.

3.5. MiR-101-3p shared the targets with RUSC1-AS1 and Notch1

To probe the interaction between RUSC1-AS1 and Notch1, we searched the miRNA targets of RUSC1-AS1 through online database Starbase (http://starbase.sysu.edu.cn/index.php), meanwhile, the upstream targets of Notch1 were also searched in online databases, including miRmap (http://mirnamap.mbc.nctu.edu.tw/), microT (http://mirtarbase.mbc.nctu.edu.tw/index.html), miRanda (http://www.microrna.org/microrna/home.do) and Targetscan (http://www.targetscan.org/vert_72/). It was found that miR-101-3p shared the targets with RUSC1-AS1 and Notch1 (Fig. 5 A and B). Next, we carried out qRT-PCR to evaluate miR-101-3p levels in OS tissues. The results represented that miR-101-3p expression in OS carcinoma was significantly down-regulated ($P < 0.05$, Fig. 5C). To clarify the targeting relationship between miR-101-3p and RUSC1-AS1, miR-101-3p and Notch1, we conducted the dual luciferase activity experiment and RIP assay. The results showed that miR-101-3p considerably inhibited luciferase activity of OS cells transfected with RUSC1-AS1-WT and Notch1-WT, while had no obvious effect on RUSC1-AS1-MUT and Notch1-MUT-transfected cells ($P > 0.05$, Fig. 5D and F). RIP experimental statistics illustrated that after the transfection with miR-101-3p mimics, the precipitated amounts of RUSC1-AS1 and Notch1 in the Ago2 antibody group were higher than those in the IgG group, suggesting that RUSC1-AS1 and Notch1 were bound to Ago2 protein by miR-101-3p ($P < 0.05$, Fig. 5E and G). The above results confirmed that RUSC1-AS1 targeted miR-101-3p, and Notch1 was a functional target of miR-101-3p.

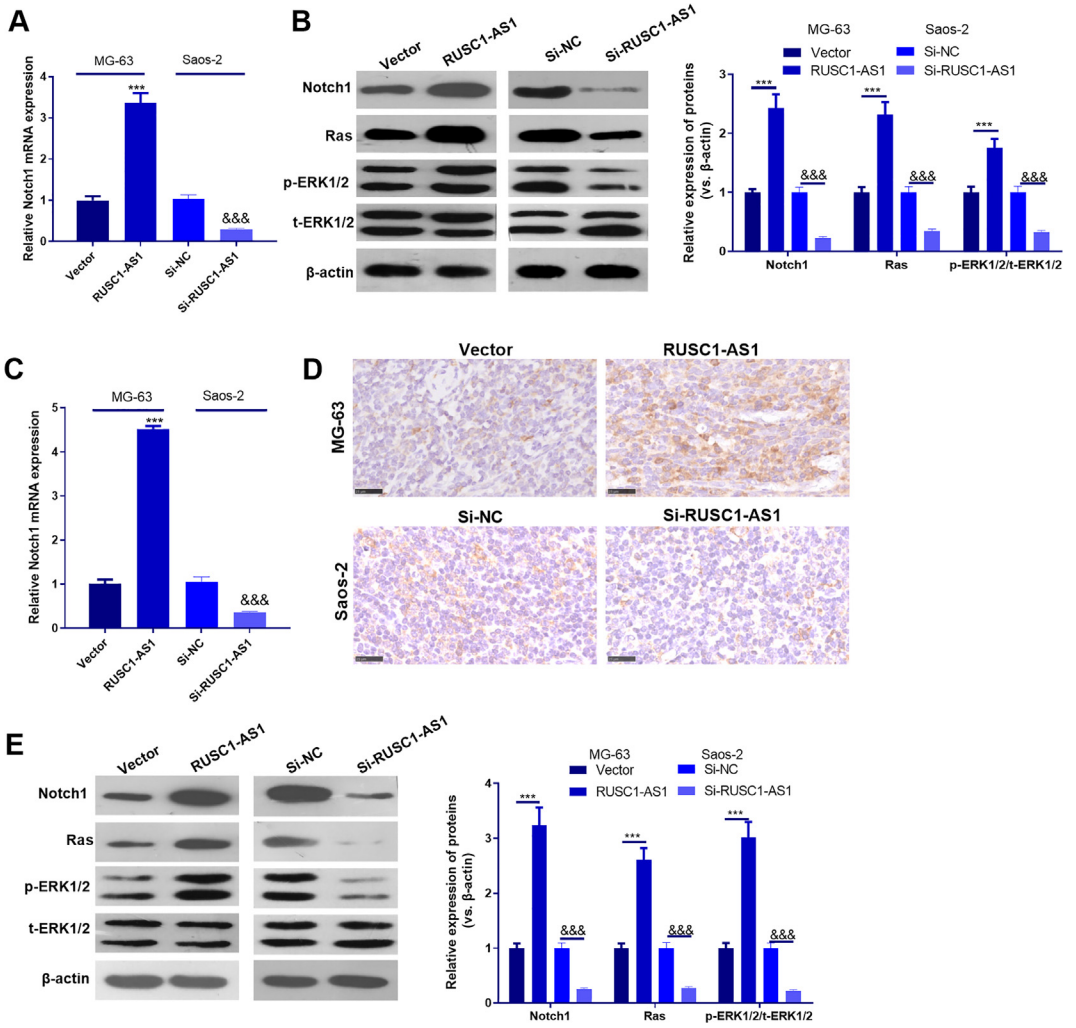

Fig. 4. RUSC1-AS1 promoted Notch1 expression. MG-63 cells transfected RUSC1-AS1 overexpressing plasmids and Saos-2 cells transfected with Si-RUSC1-AS1. A: Notch1 mRNA relative expression in MG-63 cells and Saos-2 cells were detected by via qRT-PCR. B: Western blot was employed to analyze Notch1-Ras-ERK1/2 proteins. *** $P < 0.001$, (vs. Vector group), &&& $P < 0.001$ (vs. Si-NC group). N = 3. C: qRT-PCR was applied to measure Notch1 mRNA relative expression in tumorigenic tissues. D: IHC was carried out to detect Notch1 expression in the tumor tissues. E: Western blot was employed to analyze Notch1-Ras-ERK1/2 proteins in the tumor tissues. *** $P < 0.001$, (vs. Vector group), &&& $P < 0.001$ (vs. Si-NC group). N = 4.

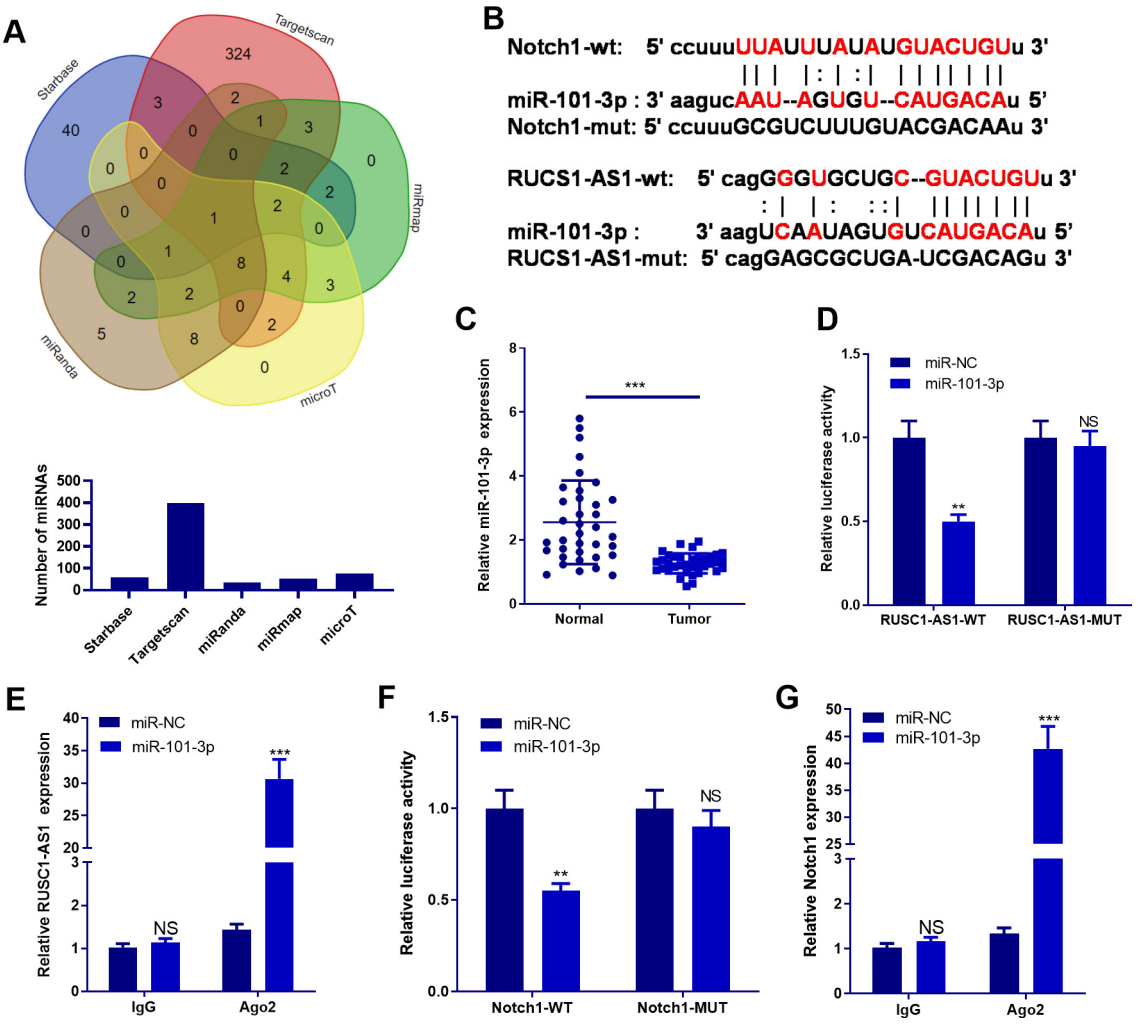

Fig. 5. MiR-101-3p was the target of RUSC1-AS1 and Notch1. A. The miRNA targets of RUSC1-AS1 through online database Starbase, the upstream miRNA targets of Notch1 were also searched in online databases, including miRmap, microT, miRanda and Targetscan, Venn diagram was used to analyze the common miRNA targets of RUSC1-AS1 and Notch1. B. The base binding relationships between RUSC1-AS1 and miR-101-3p, miR-101-3p and Notch1. C: qRT-PCR was applied to examine miR-101-3p expression in adjacent tissues and OS tissues. *** P < 0.001. D-E: Dual luciferase reporter gene assay and RIP assay were used to confirm the binding relationship between RUSC1-AS1 and miR-101-3p. F-G: Dual luciferase reporter gene assay and RIP assay were used to confirm the binding relationship between Notch1 and miR-101-3p. ** P < 0.01, *** P < 0.001 (vs.miR-NC), NS P > 0.05 (vs. miR-NC). N = 3.

3.6. miR-101-3p downregulated Notch1 and inactivated Ras-ERK pathway

To study the effect of RUSC1-AS1-miR-101-3p in regulating OS progression, MG-63 cells were transfected with miR-101-3p mimics and/or RUSC1-AS1 overexpressing plasmids. The level of miR-101-3p was detected by qRT-PCR, which resulted out that miR-101-3p level was markedly increased by miR-101-3p mimics transfection, while miR-101-3 was obviously attenuated by overexpressing RUSC1-AS1 ($p < 0.05$ compared with miR-101-3p group, Fig. 6 A), indicating that RUSC1-AS1 repressed miR-101-3p in MG-63 cells. However, miR-101-3p had no obvious effect on RUSC1-AS1 expression (Fig. 6B). Next, the level of Notch1 and Ras-ERK pathway were detected by qRT-PCR and western blot respectively. As a result, Notch1 and Ras-ERK pathway were both inhibited following miR-101-3p upregulation, however, forced RUSC1-AS1 expression blocked miR-101-3p mediated inhibitory effect on Notch1 and Ras-ERK pathway (Fig. 6C and D). Furthermore, we transfected MG-63 cells with Notch1 overexpression plasmids and/or miR-101-3p mimics. The results of qRT-PCR and western blot showed that Notch1 overexpression enhanced Ras and ERK1/2 phosphorylation. However, compared with the Notch1 group, miR-101-3p mimics transfection resulted in lower level of Notch1 and Ras-ERK pathway ($p < 0.05$ vs. Notch1 group, Fig. 6E). Taken together, those data suggested that RUSC1-AS1 promoted Notch1-mediated Ras-ERK pathway activation via inhibiting miR-101-3p.

3.7. RUSC1-AS1 blocked miR-101-3p mediated effects in OS cells

To study the effect of RUSC1-AS1/miR-101-3p axis in regulating OS progression, we detected the malignant behaviors of MG-63 cells transfected with miR-101-3p mimics and/or RUSC1-AS1 overexpressing plasmids. The results suggested that compared with the NC group, miR-101-3p upregulation inhibited tumor cell proliferation, promoted apoptosis, attenuated the tumor cell migration and invasion (Fig. 7 A-E). However, over-expressing RUSC1-AS1 in miR-101-3p mimics transfected cells enhanced cell proliferation, mitigated apoptosis, aggravated cell migration and invasion in comparison with miR-101-3p group (Fig. 7A–E). Besides, western blot experiments statistics revealed that E-cadherin level in the miR-101-3p group was increased, and N-cadherin, Vimentin and Snail protein levels were decreased (Fig. 7F). Similarly, RUSC1-AS1 overexpression mostly reversed miR-101-3p-mediated effects in

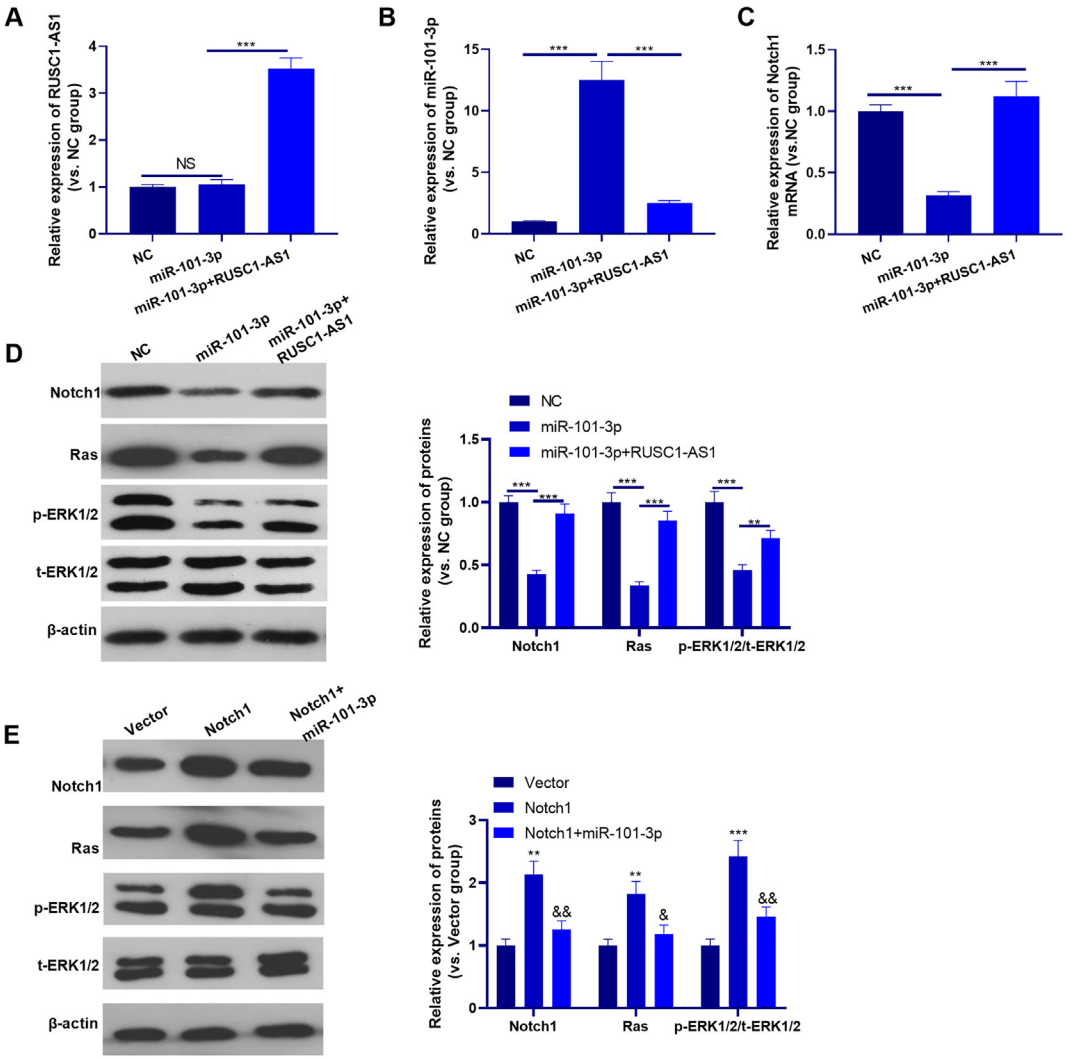

Fig. 6. RUSC1-AS1 targeted miR-101-3p to regulate Notch1 expression. A-C.MG-63 cells were transfected with miR-101-3p mimics and/or RUSC1-AS1 overexpressing plasmids. The levels of miR-101-3p (A), RUSC1-AS1 (B) and Notch1 (C) were detected by qRT-PCR. D. The level of Notch1 and Ras-ERK pathway were detected by western blot. E. MG-63 cells were transfected with Notch1 overexpression plasmids and/or miR-101-3p mimics. The levels of Notch1 and Ras-ERK pathway were detected by western blot. NS $P > 0.05$, ** $P < 0.01$, *** $P < 0.001$. && $P < 0.01$, &&& $P < 0.001$ (vs. Notch1 group). N = 3.

modulating EMT (Fig. 7F). These results further confirmed that miR-101-3p restrained OS cell proliferation, migration and invasion, and those effects were weakened by RUSC1-AS1 (Fig. 8).

4. Discussion

In this research, we unveiled that RUSC1-AS1 expression was raised and associated with worse clinical outcomes in OS patients. Over-expressed RUSC1-AS1 enhanced cell proliferation, migration and invasion *in vitro* and *in vivo* and accelerated tumor growth *in vivo*. Additionally, this study manifested that RUSC1-AS1 upregulation enhanced Notch1/Ras-ERK pathway expression by inhibiting miR-101-3p.

Long non-coding RNA (lncRNA) makes great contribution to OS tumor growth and metastasis regulation [22]. For instance, Linc00460 was raised in OS tissues and cells, and its high expression was positively correlated with OS patients' distant metastasis and poor overall survival rate of OS patients, and its down-regulation inhibited OS cell proliferation and metastasis *in vitro* [23]. LncRNA FBXL19-AS1 was increased in OS tissues and cell lines, and it was proved promoting OS cell proliferation, migration and invasion in experiments *in vitro* [24]. RUSC1-AS1, a novel long non-coding RNA, has been proved to monitor tumor development by regulating cancer cell proliferation, migration, apoptosis, and invasion pathways. For example, RUSC1-AS1 was upregulated and associated with overall survival (OS) of laryngeal squamous cell carcinoma (LSCC) [25]. In another study, RUSC1-AS1 inhibition restrained cervical cancer cell proliferation, migration, and invasion and impeded tumor growth *in vivo* [15]. Here, we observed that RUSC1-AS1 was also overexpressed in OS tissues and cells and promoted the malignant behaviors of OS cells. Clinically, RUSC1-AS1 overexpression was associated with poorer pathological indexes of OS patients. Therefore, those data proved that RUSC1-AS1 exerts a carcinogenic effect in OS.

Researches have unveiled that long non-coding RNA (lncRNA) can be used as competitive endogenous RNA (ceRNA) to bind to the same miRNA as the mRNA competitor. This interaction between lncRNA, miRNA and mRNA is called ceRNA crosstalk [26]. For instance, Jin et al. found that lncRNA SND1-IT1 accelerated OS proliferation and migration by sponging miRNA-665 and regulating POU2F1, thus stimulating OS development [27]. Similar mechanism was also found in RUSC1-AS1 [15]. Based on these studies, we hypothesized that RUSC1-AS1 might act as ceRNA in the OS, so we looked for potential interactions with miRNAs via

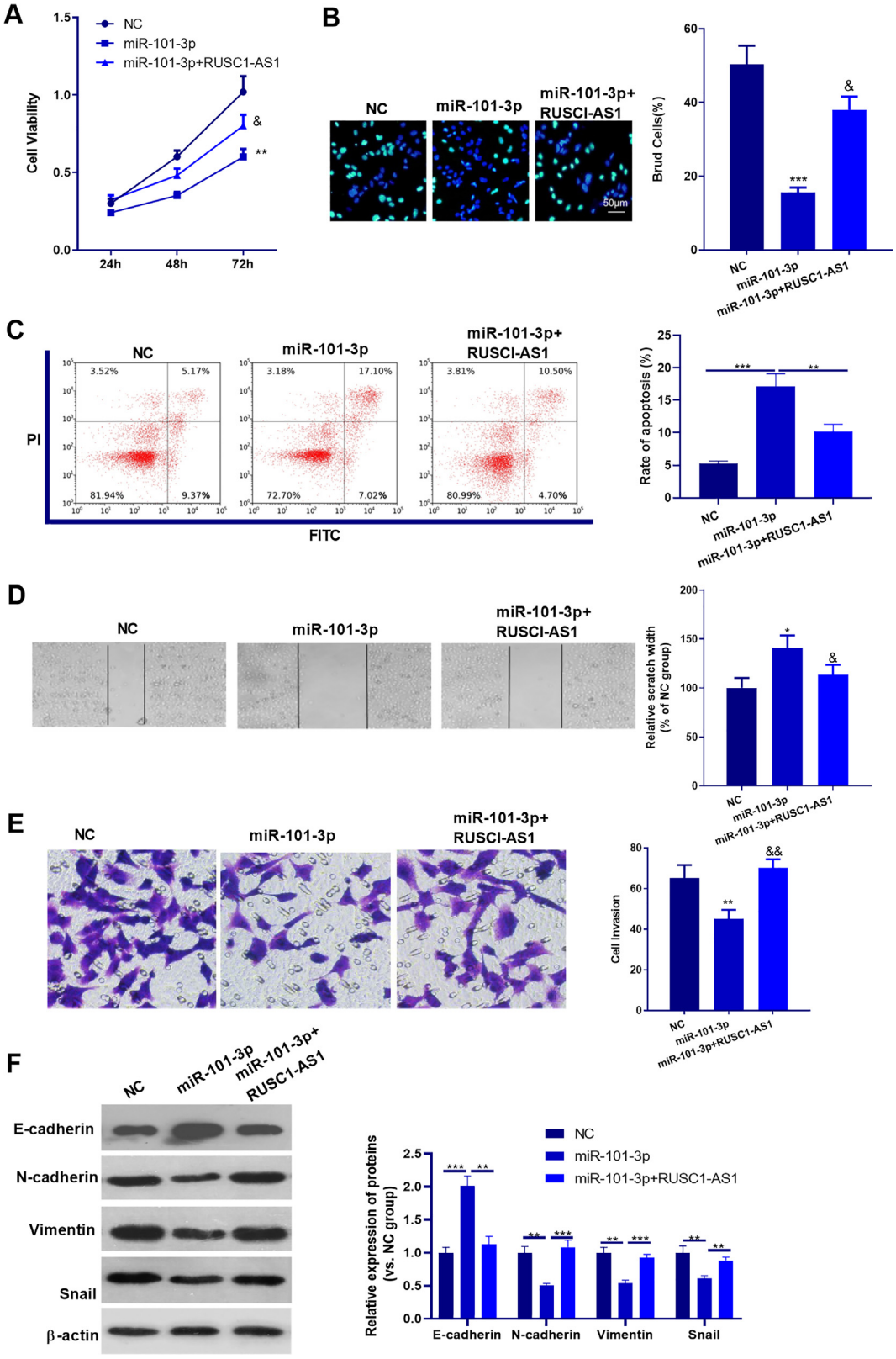

Fig. 7. miR-101-3p overexpression inhibited tumor proliferation and metastasis and RUSC1-AS1 reversed miR-101-3p-mediated effects. MG-63 cells were transfected with miR-101-3p mimics and/or RUSC1-AS1 overexpressing plasmids. A-B: CCK8 assay (A) and BrdU assay (B) were performed to detect cell proliferation. C. The apoptosis rate of the cells was examined by flow cytometry. D and E. Wounding healing test (D) and Transwell assay (E) for migration and invasion determination. F: The EMT markers including E-cadherin, N-cadherin, Snail and Vimentin were examined via Western blot. * $P < 0.03$, ** $P < 0.01$, *** $P < 0.001$ (vs. NC group). & $P < 0.05$, && $P < 0.01$, &&& $P < 0.001$ (vs. miR-101-3p group). N = 3.

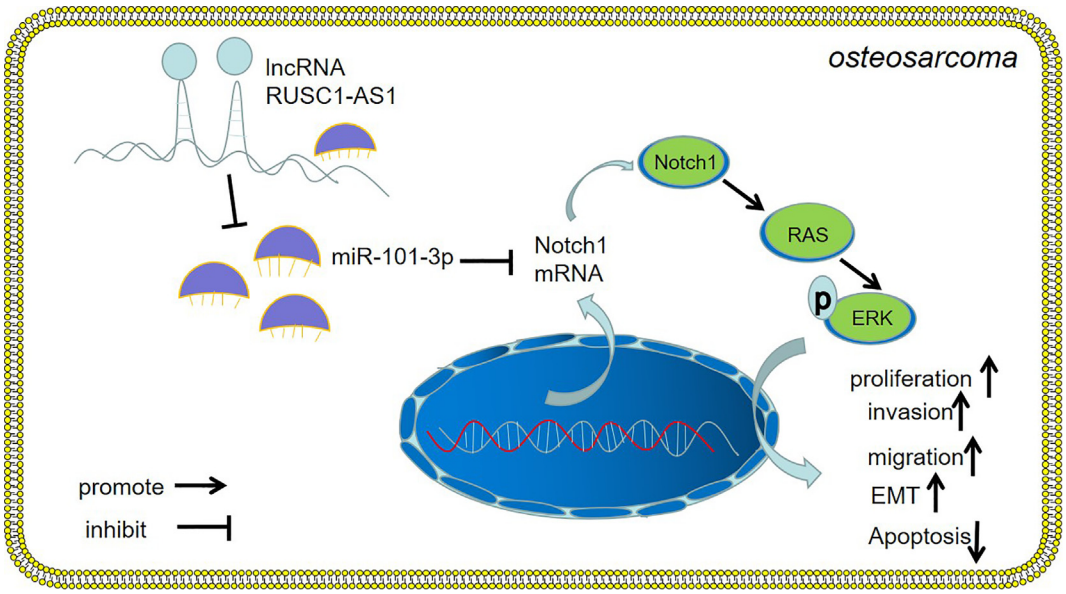

Fig. 8. The diagrammatic sketch of RUSC1-AS1-miR-101-3p-Notch1-Ras-ERK1/2 axis in OS progression.

bioinformatics analysis. It was found that miR-101-3p was a ceRNA of RUSC1-AS1. Functionally, miR-101-3p inhibited OS progression, while RUSC1-AS1 upregulation blocked miR-101-3p-mediated effects. Hence, RUSC1-AS1 influences OS growth by sponging miR-101-3p (Fig. 8).

Notch family members have been proved to exert crucial roles in skeletal physiology and disease [28]. Recently, increasing evidence suggest that Notch signaling pathways are upregulated in OS and function a great role. For instance, Notch1, one member of Notch genes, was upregulated in OS tumor, and high tumor expression of intercellular domain (NICD1) and the Notch target gene Hes1 correlated with poor chemotherapy response [29]. Besides, Notch1 induces multidrug resistance of hypoxic OS cells through regulating MRP1 gene expression [30]. Several chemical drugs, such as Diallyl trisulfide [31] and Curcumin [32] inhibit OS proliferation, invasion and angiogenesis and promote apoptosis dependently via repressing Notch1 pathway. Interestingly, recent studies also verified that the lncRNA-miRNA axis modulates tumor development by Notch1 pathway. For example, lncRNA CRNDE activates Notch1 signaling in OS, thus promoting the proliferation, invasion, migration and epithelial-mesenchymal transition of OS cell [33]. Interestingly, RUSC1-AS1, which was upregulated in HCC tissues and cells, and predicted unfavorable prognosis of HCC patients, upregulates NOTCH3 and to trigger the NOTCH signaling pathway [34]. Presently, we found that Notch1 was also upregulated in OS and had a positive relationship with RUSC1-AS1. Gain- and loss- of functional assays authenticated that RUSC1-AS1 aggravated OS development via activating Notch1 pathway.

Mitogen-Activated Protein Kinases (MAPKs) are evolutionarily conserved components in mammals. The Ras-ERK pathway has been recognized as one of the crucial pathways [35]. In tumor progression, the activation of Ras-ERK axis is associated with enhanced migration, epithelial to mesenchymal transition (EMT) and increased matrix metalloproteinase 2/9 activity of cancer cells [36]. In a mouse OS model, downregulation of the Ras/MEK/ERK and Ras/PI3K/Akt pathways markedly reduces the angiogenic factors expression of bFGF, HGF, and TGF-β [37]. Mittal S et al. Showed that in breast cancer, Notch pathway may co channel with Ras/MAPK pathway in the pathogenesis of breast cancer [38]. Basing the above researches, we also explored the role of Ras/ERK signaling pathway in OS. On the other hand, we have a clear understanding of the expression and role of Notch1 in OS, but the specific mechanism is still unclear. In our study, we found that RAS-ERK1/2 was also upregulated following the upregulation of RUSC1-AS1. While inhibiting Notch1 whether by knocking down RUSC1-AS1 or upregulating miR-101-3p significantly inactivated RAS-ERK1/2 pathway. Therefore, RUSC1-AS1 promotes OS development via the miR-101-3p-Notch1-Ras-ERK signaling pathway.

To sum up, we determined that over-expressed RUSC1-AS1 is a carcinogenic lncRNA that plays a vital role in the OS process. The present study initially manifested the effect of the RUSC1-AS1 / miR-101-3p/Notch1-RAS-ERK1/2 pathway in OS, and revealed that silencing RUSC1-AS1 inhibits OS progression by up-regulating miR-101-3p, which could provide a new therapeutic target for OS.

5. Ethics statementss

Our study was approved by the Ethics Review Board of The Second Hospital of Jilin University.

6. Data Availability Statement

The data sets used and analyzed during the current study are available from the corresponding author on reasonable request.

Funding

This research did not receive any specific grant from funding agencies in the public, commercial, or not- for- profit sectors.

Declaration of Competing Interest

The authors declare that they have no known competing financial interests or personal relationships that could have appeared to influence the work reported in this paper.

References

[1] W. Linyi, W. Lijuan, Z. Xinhua, Knockdown of lncRNA HOXA-AS2 Inhibits viability, migration and invasion of OS cells by miR-124-3p/E2F3, Oncol. Targets Ther. 12 (2019) 10851–10861.

[2] N. Montazeri-Najafabady, M.H. Dabbaghmanesh, N. Chatrabnous, M.R. Arabnezhad, The Effects of astaxanthin on proliferation and differentiation of MG-63 osteosarcoma cells via aryl hydrocarbon receptor (AhR) pathway: a comparison with AhR endogenous ligand, Nutr. Cancer 72 (8) (2020) 1400–1410.
[3] J. Fellenberg, B. Lehner, H. Saehr, A. Schenker, P. Kunz, Tumor suppressor function of miR-127-3p and miR-376a-3p in osteosarcoma cells, Cancers (Basel) 11 (12) (2019) 2019.
[4] X. Wang, L. Peng, X. Gong, X. Zhang, R. Sun, LncRNA HIF1A-AS2 promotes osteosarcoma progression by acting as a sponge of miR-129-5p, Aging (Albany NY) 11 (24) (2019) 11803–11813.
[5] Q. Wang, G. Yan, Corrigendum: IDLDA: an improved diffusion model for predicting LncRNA-disease associations, Front Genet. 11 (2020) 137.
[6] Q. Huang, S.-Y. Shi, H.-b. Ji, S.-X. Xing, LncRNA BE503655 inhibits osteosarcoma cell proliferation, invasion/migration via Wnt/β-catenin pathway, Biosci. Rep. 39 (7) (2019), https://doi.org/10.1042/BSR20182200.
[7] Y. Wang, N. Liu, M.Y. Li, M.F. Du, Long non-coding RNA ZEB2-AS1 regulates osteosarcoma progression by acting as a molecular sponge of miR-107 to modulate SALL4 expression, Am. J. Transl. Res. 13 (3) (2021) 1140–1154.
[8] C.C. Hu, Y.W. Liang, J.L. Hu, L.F. Liu, J.W. Liang, R. Wang, LncRNA RUSC1-AS1 promotes the proliferation of breast cancer cells by epigenetic silence of KLF2 and CDKN1A, Eur. Rev. Med. Pharmacol. Sci. 23 (15) (2019) 6602–6611.
[9] M. Correia de Sousa, M. Gjorgjieva, D. Dolicka, C. Sobolewski, M. Foti, Deciphering miRNAs' action through miRNA editing, Int. J. Mol. Sci. 20 (24) (2019) 6249, https://doi.org/10.3390/ijms20246249.
[10] Y. Meng, R. Gao, J. Ma, et al., MicroRNA-140-5p regulates OS chemoresistance by targeting HMGN5 and autophagy, Sci. Rep. 7 (1) (2017) 416.
[11] Y. Xu, T. Ji, N. An, X. Wang, H. Zhang, F. Xu, LINC00943 is correlated with gastric cancer and regulates cancer cell proliferation and chemosensitivity via hsa-miR-101-3p [published online ahead of print, 2021 Jun 4], Int. J. Clin. Oncol. (2021), https://doi.org/10.1007/s10147-021-01945-5.
[12] R. Jiang, C. Zhang, G. Liu, R. Gu, H. Wu, MicroRNA-101 inhibits proliferation, migration and invasion in OS cells by targeting ROCK1, Am. J. Cancer Res. 7 (1) (2017) 88–97.
[13] L. Zhu, Y. Chen, K. Nie, Y. Xiao, H. Yu, MiR-101 inhibits cell proliferation and invasion of pancreatic cancer through targeting STMN1, Cancer Biomark. 23 (2) (2018) 301–309.
[14] S. Zhang, L. Ding, F. Gao, H. Fan, Long non-coding RNA DSCAM-AS1 upregulates USP47 expression through sponging miR-101-3p to accelerate OS progression, Biochem. Cell Biol. (2020), https://doi.org/10.1139/bcb-2020-0031.
[15] Q. Guo, Q. Zhang, L. Lu, Y. Xu, Long noncoding RNA *RUSC1-AS1* promotes tumorigenesis in cervical cancer by acting as a competing endogenous RNA of microRNA-744 and consequently increasing Bcl-2 expression, Cell Cycle 19 (10) (2020) 1222–1235.
[16] O. Meurette, P. Mehlen, Notch signaling in the tumor microenvironment, Cancer Cell. 34 (4) (2018) 536–548.
[17] K.N. Lovendahl, S.C. Blacklow, W.R. Gordon, The molecular mechanism of notch activation, Adv Exp. Med. Biol. 1066 (2018) 47–58.
[18] R.-H. Gan, H. Wei, J. Xie, D.-P. Zheng, E.-L. Luo, X.-Y. Huang, J. Xie, Y. Zhao, L.-C. Ding, B.-H. Su, L.-S. Lin, D.-L. Zheng, Y.-G. Lu, Notch1 regulates tongue cancer cells proliferation, apoptosis and invasion, Cell Cycle 17 (2) (2018) 216–224.
[19] M.A. Rice, E.-C. Hsu, M. Aslan, A. Ghoochani, A. Su, T. Stoyanova, Loss of notch1 activity inhibits prostate cancer growth and metastasis and sensitizes prostate cancer cells to antiandrogen therapies, Mol. Cancer Ther. 18 (7) (2019) 1230–1242.
[20] L.u. Qian, W. Zhang, B.o. Lei, A. He, L. Ye, X. Li, X. Dong, MicroRNA-101 regulates T-cell acute lymphoblastic leukemia progression and chemotherapeutic sensitivity by targeting Notch1, Oncol. Rep. 36 (5) (2016) 2511–2516.
[21] X. Xiao, Y. Zhang, W. Pan, F. Chen, miR-139-mediated NOTCH1 regulation is crucial for the inhibition of OS progression caused by resveratrol, Life Sci. 242 (2020) 117215.
[22] W. Jin-Yan, Y. Yan, M.a. Yajun, et al., Potential regulatory role of lncRNA-miRNA-mRNA axis in OS, Biomed. Pharmacother. 121 (2020) 109627.
[23] L. Hongkai, X. Panpan, Y. Ningwei, et al., Linc00460 promotes OS progression via miR-1224-5p/FADS1 axis, Life Sci. 233 (2019) 116757.
[24] P. Runsang, H.e. Zhixu, R. Wanyuan, et al., lncRNA FBXL19-AS1 regulates OS cell proliferation, migration and invasion by sponging miR-346, Oncol. Targets Ther. 11 (2018) 8409–8420.
[25] L. Hui, J. Wang, J. Zhang, J. Long, lncRNA TMEM51-AS1 and RUSC1-AS1 function as ceRNAs for induction of laryngeal squamous cell carcinoma and prediction of prognosis, PeerJ. 7 (2019) e7456, https://doi.org/10.7717/peerj.7456.
[26] C. Lan, H. Peng, G. Hutvagner, J. Li, Construction of competing endogenous RNA networks from paired RNA-seq data sets by pointwise mutual information, BMC Genomics 20 (S9) (2019), https://doi.org/10.1186/s12864-019-6321-x.
[27] X.-M. Jin, B. Xu, Y. Zhang, et al., LncRNA SND1-IT1 accelerates the proliferation and migration of OS via sponging miRNA-665 to upregulate POU2F1, Eur. Rev. Med. Pharmacol. Sci. 23 (2019) 9772–9780.
[28] E. Canalis, Notch in skeletal physiology and disease, Osteoporos Int. 29 (12) (2018) 2611–2621.
[29] L. Yu, K. Xia, T. Gao, et al., The notch pathway promotes os progression through activation of ephrin reverse signaling, Mol. Cancer Res. 17 (12) (2019) 2383–2394.
[30] C. Li, D. Guo, B. Tang, Y. Zhang, K. Zhang, L. Nie, Notch1 is associated with the multidrug resistance of hypoxic OS by regulating MRP1 gene expression, Neoplasma 63 (5) (2016) 734–742.
[31] Y. Li, J. Zhang, L. Zhang, M. Si, H. Yin, J. Li, Diallyl trisulfide inhibits proliferation, invasion and angiogenesis of OS cells by switching on suppressor microRNAs and inactivating of Notch-1 signaling, Carcinogenesis 34 (7) (2013) 1601–1610.
[32] Y. Li, J. Zhang, D. Ma, et al., Curcumin inhibits proliferation and invasion of OS cells through inactivation of Notch-1 signaling, FEBS J. 279 (12) (2012) 2247–2259.
[33] Z. Li, Y. Tang, W. Xing, W. Dong, Z. Wang, LncRNA, CRNDE promotes OS cell proliferation, invasion and migration by regulating Notch1 signaling and epithelial-mesenchymal transition, Exp. Mol. Pathol. 104 (1) (2018) 19–25.
[34] Y.A. Chen, L. Cheng, Y. Zhang, L. Peng, H.G. Yang, LncRNA RUSC1-AS1 promotes the proliferation of hepatocellular carcinoma cells through modulating NOTCH signaling, Neoplasma 67 (06) (2020) 1204–1213.
[35] Y.H. Li, Y.X. Li, M. Li, et al., The Ras-ERK1/2 signaling pathway regulates H3K9ac through PCAF to promote the development of pancreatic cancer, Life Sci. 256 (2020) 117936.
[36] Q. Ma, H. Wu, Y. Xiao, Z. Liang, T. Liu, Upregulation of exosomal microRNA–21 in pancreatic stellate cells promotes pancreatic cancer cell migration and enhances Ras/ERK pathway activity, Int. J. Oncol. 56 (4) (2020) 1025–1033.
[37] M. Tsubaki, Y. Yamazoe, M. Yanae, et al., Blockade of the Ras/MEK/ERK and Ras/PI3K/Akt pathways by statins reduces the expression of bFGF, HGF, and TGF-β as angiogenic factors in mouse OS, Cytokine 54 (1) (2011) 100–107.
[38] S. Mittal, D. Subramanyam, D. Dey, R.V. Kumar, A. Rangarajan, Cooperation of Notch and Ras/MAPK signaling pathways in human breast carcinogenesis, Mol. Cancer 8 (1) (2009) 128, https://doi.org/10.1186/1476-4598-8-128.